

Preparation and characterization of a new derivative of rhodamine B with an alkoxysilane moiety

T. Nedelčev*, D. Račko, I. Krupa

Polymer Institute, The Slovak Academy of Sciences (SAS), Dúbravská cesta 9, 842 36 Bratislava, Slovakia

Received 11 September 2006; accepted 9 November 2006

Available online 26 December 2006

Abstract

The synthesis of a novel rhodamine B derivative carrying an alkoxysilane moiety (RBS) is described. Rhodamine B (RB) was attached to the Si atom by an amide linkage to provide the functionalized silane via the condensation of 3-aminopropyltriethoxysilane (APTES) with RB by azeotropic distillation in water. The physical properties and structure of RBS were characterized using ^1H NMR, ^{13}C NMR, HH COSY, FTIR, UV–vis measurements spectra and Kofler's apparatus. The absorbance of RBS was 1.6 times higher than that of RB. The equilibrium conformation of the RBS molecule was determined by means of a molecular simulation study; spectral properties are discussed based on the obtained computational results.

© 2006 Elsevier Ltd. All rights reserved.

Keywords: Rhodamine B; Silane; Fluorescence; Simulation

1. Introduction

Rhodamines have been the subject of longstanding research. They are xanthene derivatives of alkylated *m*-aminophenols which fluoresce due to their stiff molecular structure which prevents the energy of the excited state from being lost by torsional vibration [1]. The first synthesis of rhodamine B was performed by Noelting and Dziewonski [2] in 1905 who found that the two principal forms of rhodamine B are the lactone (RBL) and salt form (RB).

In polar solvents, the colourless RBL form is transformed into the violet coloured zwitterion (RB^{+-}). To the carboxyl group formed by the opening of the lactone ring of RBL, a proton can be added, forming RBH^+ that has nearly the same absorption spectrum as RB^{+-} . Anions such as chloride, bromide and perchlorate form ion pairs in solution with the rhodamine cation; hence, the ion pair molecules have the same absorption spectra as the free cation [3].

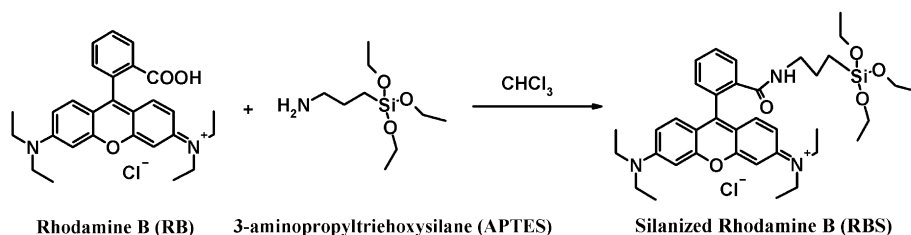
Electron transfer from the xanthene part of the molecule to the phthalide results in a charge-transfer (CT) excited state, the excited RB^{+-} [4]. Radiation-less deactivation pathways for zwitterionic and/or cationic forms of rhodamines were studied by Drexhage [5] who postulated that torsional motion of the diethylamino groups in rhodamine B is involved in non-radiative processes. Rhodamine 101 contains alkyl-amino groups rigidly linked to the xanthene skeleton. The compound's very high luminescence quantum yield, and in particular, the independency of this quantum yield on temperature, seemed to be very strong arguments confirming that this model explains the nature of the non-radiative decay [3].

Guo et al. [6] studied the photocatalytic degradation of rhodamine B on a SiW_{11}Ni support and found that the dye underwent deethylation, deamination, decarboxylation, and cleavage of the chromophore ring structure, resulting in the final products of CO_2 , NO_3^- , and Cl^- ions.

Many investigations have been carried out on the physical and chemical properties of rhodamines. Their optical properties depend on many factors, such as solvent (polarity and aprotic character), concentration and pH [7–9]. The ethyl ester of rhodamine B (*rhodamine 6G*) was used in one of the first dye lasers

* Corresponding author. Fax: +421 2 5477 5923.

E-mail address: upoltned@savba.sk (T. Nedelčev).



Scheme 1. The condensation reaction between APTES and RB in chloroform.

and it remains a commonly used laser dye [10]. Rhodamine B has been found to lase in alcohol, water, and PMMA [11–14].

As the concentrations of RB^{+-} and RBH^+ increase, dimerization [15] occurs, causing an apparent deviation from Lambert–Beer's law. Dimerization of rhodamine B and rhodamine 6G leads not only to non-Lambert–Beer's law absorption, but also is detrimental to laser action [16]. Formation of the simplest dimeric aggregate involves dye–dye interactions negate monomer solvation [17]. A low dielectric constant non-polar solvent favours the formation of dimers [18,19].

In a polar solvent, such as ethanol, the carboxylic group of the rhodamines participates in a typical acid–base equilibrium [20]. The lactone form of rhodamine B which is colourless shows no emission because the dye's π -electron system is interrupted [7]. However, rhodamine 6G is unable to lactonize due to the ester form of the carboxylic group [21]. The main band of rhodamine B [22], corresponding to the monomer, occurs at 542.5 nm and its shoulder represents the dimer [23]. Recently, other important novel applications of rhodamines in the acid or ester form have been reported, such as their use as probes and indicators [24–26] and as dyes for medical and biological applications [27–29].

The reaction between the carboxylic group of rhodamines and amines have attracted little interest; Roy et al. [30] used Et_3N as catalyst for the condensation of the carboxylic group of rhodamine B with *N*-mono(*tert*-butoxycarbonyl)ethylene-diamine in acetonitrile. The reaction time was 10 h at a temperature of 20 °C and gave a yield of 81%. Ficht et al. [31] used *N,N'*-diisopropylcarbodiimide as a water-binder and *N*-ethyl-diisopropylamine as catalyst in the condensation reaction between the carboxylic group of rhodamine S and phenethylamine; the yield of the prepared amide was 63%. Shukla et al. [32] used *N,N'*-dicyclohexylcarbodiimide as a water-binding agent and DMAP as catalyst during a 5-h reaction at 20 °C, giving a yield of 65%. The preparation of a rhodamine B derivative carrying ethoxy-silano groups was described by Ohishi [33] who reacted sulforhodamine B with SOCl_2 in pyridine to produce the sulfonamide bond.

The study of the structure of rhodamines B and 6G, using molecular simulation methods, employing both semi-empirical and *ab initio* calculations, revealed that the xanthene and phthalide parts of the molecule formed perpendicular and *gauche* angles [15].

The aim of this paper is to present a simple method for the preparation of a new rhodamine B derivative that carries ethoxy-silano groups, without loss of optical character. A condensation reaction has been employed for the preparation of the

product RBS (Scheme 1); the structure of RBS was confirmed by FTIR, ^1H NMR, ^{13}C NMR and HH COSY spectral measurements. Optical properties are discussed and a simple molecular simulation study was performed.

2. Experimental

2.1. Materials and measurements

Rhodamine B was obtained from Fluka, 3-aminopropyltriethoxysilane from Degussa and chloroform p.a. from AFT Bratislava. FTIR spectra were recorded on a Nicolet FTIR 400 spectrometer, ^1H NMR spectrum recorded on a Bruker 300 MHz and HH COSY spectrum was recorded on a Bruker 600 MHz NMR spectrometer. UV spectra were measured on a Shimadzu UV-1650 PC. Fluorescence emission was measured using a Perkin–Elmer MPF-4. Measurements of boiling points were performed on a Nagema PHMG 05 Kofler's hot stage apparatus.

2.2. Molecular modeling

The structure of the RBS was investigated by means of molecular modeling methods employing semi-empirical calculations [34,35]. The equilibrium conformer was obtained on the basis of an exploration of 2000 structures. The starting coordinates of the explored conformers were generated by a Monte Carlo algorithm within an energy window of 10 kcal/mol.

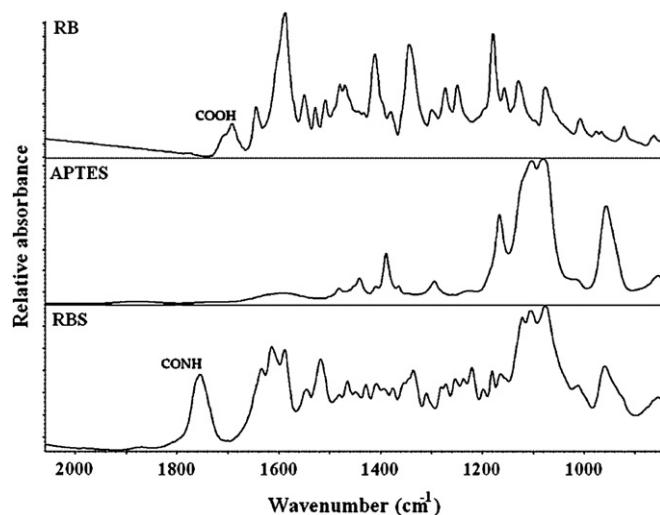


Fig. 1. FTIR spectra of RB, APTES and RBS.

The convergence criteria were set to 1×10^{-3} kcal/mol for energy or 1×10^{-4} Å for RMS, respectively.

2.3. Synthesis

2.3.1. 2-(3-(Diethylamino)-6-(diethylimino)-6H-xanthen-9-yl)-N-(3-(triethoxysilyl)propyl benzamide (RBS)

Rhodamine B (0.002 mol, 0.96 g) was dissolved in chloroform (30 ml). The solution was stirred and heated to the boiling point of chloroform. APTES (0.002 mol, 0.465 ml) was then added dropwise to the rhodamine solution under stirring. The reaction mixture was warmed and the water that was formed during the condensation reaction was distilled out via an azeotropic adapter. After 30 min, the chloroform was distilled from the reaction mixture and red crystals of RBS were formed (m.p. 65–70 °C) (100%).

$^1\text{H NMR}$: 0.68 (–CH₂–Si) C, 1.16–1.23 (O–CH₂–CH₃) A, (N–CH₂–CH₃) F, 1.85 (CH₂–CH₂–CH₂) D, 2.9 (CONH–CH₂–) E, 3.4 (N–CH₂–CH₃) G, 3.8 (O–CH₂–CH₃) B, 6.38 (Ar) M, 6.47 (Ar) N, 6.62 (Ar) L, 7.2 (Ar) K, 7.58–7.64 (Ar) I, J, 8 (Ar) H in CDCl₃.

$^{13}\text{C NMR}$: 7.6 (C–C), 12.54 (C–F), 18.3 (C–A), 21.2 (C–D), 42 (C–E), 44.7 (C–G), 58.4 (C–B), 97.2 (C–5, C–4), 107.4 (C–10, C–13), 109.1 (C–7, C–2), 125.1 (C–4'), 126 (C–6'), 129.3 to 129.6 (C–2', C–3', C–1, C–8), 133.6 (C–5', C–1'), 149 (C–9), 150.6 (C–6, C–3), 154.2 (C–11, C–12), 169.7 (C–H) in CDCl₃.

FTIR : C=O 1755 cm^{−1}, Si–O–C 1079 cm^{−1}, 1106 cm^{−1} and 1121 cm^{−1}.

UV : 545 nm ($\epsilon = 142\,000$ cm^{−1} mol^{−1} dm³) in EtOH.

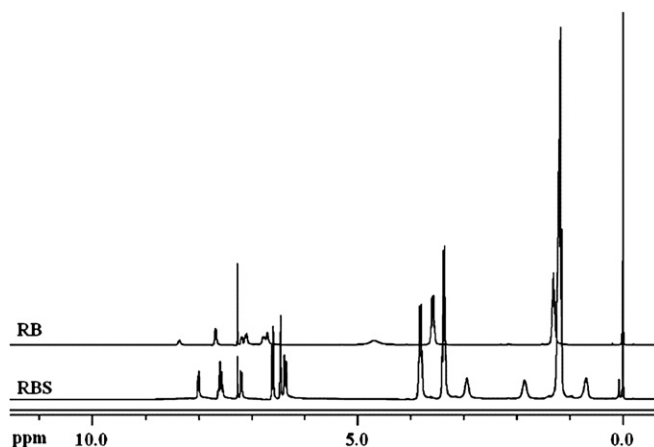


Fig. 2. $^1\text{H NMR}$ spectra of RB and RBS in CDCl₃.

3. Results and discussion

Within a condensation reaction, such as that between amines and carboxylic groups, water is produced. In the case of the condensation of APTES and RB, the by-product water had to be continuously removed from the reaction mixture in order to prevent hydrolysis of the ethoxyl groups in the aminopropyltriethoxysilane. Removal of water was performed by azeotropic distillation with chloroform. The formation of water droplets was observed in the azeotropic adapter during the first 15 min after APTES had been added; the duration

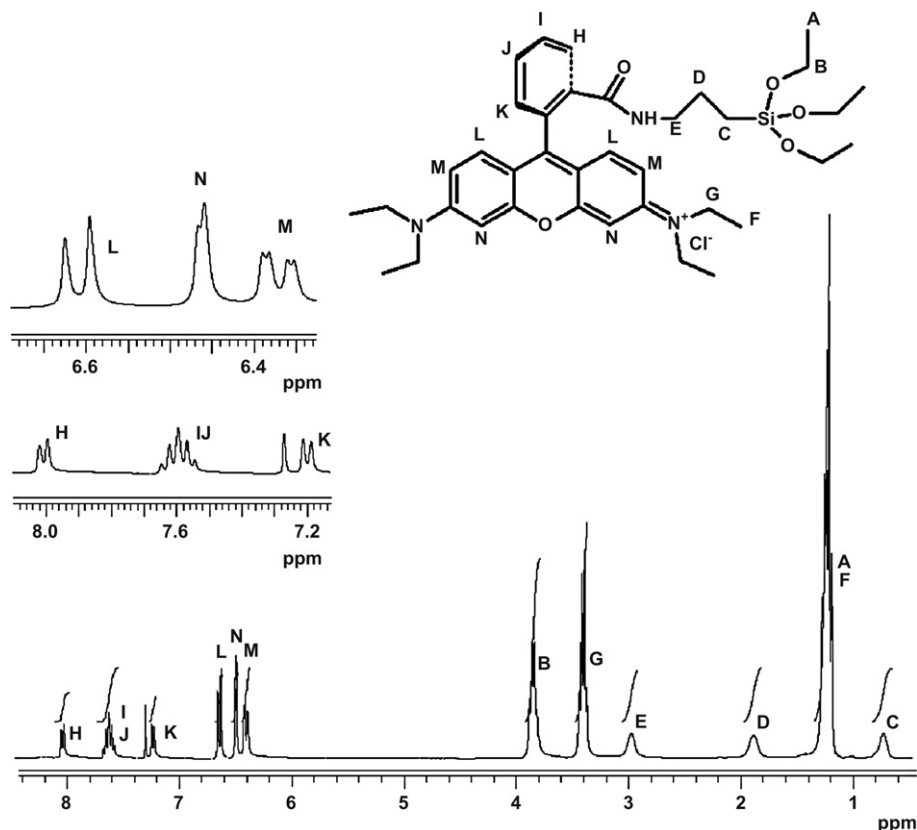


Fig. 3. $^1\text{H NMR}$ spectrum of RBS in CDCl₃.

Table 1

The comparison of theoretical and experimental integral values of signals in the ^1H NMR spectrum of RBS

Chemical shift δ (ppm)	Corresponding hydrogens	Integral values (experimental)	Integral values (theoretical)
0.675	C ($-\text{CH}_2-\text{Si}$)	2	2
1.16–1.23	A ($\text{O}-\text{CH}_2-\text{CH}_3$) F ($\text{N}-\text{CH}_2-\text{CH}_3$)	22.9	21
1.85	D ($\text{CH}_2-\text{CH}_2-\text{CH}_2$)	2.07	2
2.9	E ($\text{CONH}-\text{CH}_2-$)	1.95	2
3.4	G ($\text{N}-\text{CH}_2-\text{CH}_3$)	7.96	8
3.8	B ($\text{O}-\text{CH}_2-\text{CH}_3$)	6.18	6
6.38	M (Ar)	2.09	2
6.47	N (Ar)	1.89	2
6.62	L (Ar)	1.81	2
7.2	K (Ar)	0.97	1
7.58–7.64	I, J (Ar)	2.06	2
8	H (Ar)	1.13	1

of reaction was set to 30 min to maximize product yield (RBS).

Fig. 1 shows the FTIR spectra of RB, APTES and RBS; vibration of the carbonyl group of RB is visible at 1695 cm^{-1} . After the condensation reaction of RB with APTES the RB's carbonyl vibration shifts to 1755 cm^{-1} which indicates a change of the COOH group of RB to CONH in the product. The FTIR spectrum of RBS shows that unreacted RB was not visible. Peaks at 1079 cm^{-1} , 1106 cm^{-1} and 1121 cm^{-1} in the FTIR spectra of RBS are similar to those in the FTIR spectra of APTES; these peaks were assigned to Si–OEt vibrations.

Fig. 2 shows a comparison of the ^1H NMR spectra of RB and RBS. The $\text{CH}_3-\text{CH}_2-\text{N}$ hydrogens of RB are visible as a quartet at 3.58 ppm and the $\text{CH}_3-\text{CH}_2-\text{N}$ hydrogens of RBS as a quartet at 3.37 ppm. The chemical shift of the $\text{CH}_3-\text{CH}_2-\text{N}$ hydrogen triplet visible at 1.3 ppm in the ^1H

NMR spectrum of RB changed to 1.2 ppm in the ^1H NMR spectrum of RBS. The signals of the ethoxyl groups bound to silicon in RBS can also be observed in the ^1H NMR spectra (Fig. 3). A triplet belonging to $\text{CH}_3-\text{CH}_2-\text{O}$ hydrogens can be seen at 1.2 ppm where it is superimposed by a triplet of $\text{CH}_3-\text{CH}_2-\text{N}$ hydrogens; $\text{CH}_3-\text{CH}_2-\text{O}$ hydrogens are visible at 3.81 ppm as a quartet. The region of the RB aromatic hydrogens, which ranged from 6 to 9 ppm, differs to that of RBS (Fig. 2). Integral values calculated from the ^1H NMR spectra support the RBS structure and are summarized in Table 1.

Fig. 4 shows the ^{13}C NMR spectrum of RBS. The aliphatic carbons, labeled as A, B, C, D, E, F, G in the area from 0 to 60 ppm of the spectrum were assigned unambiguously. Identification of the signals in the aromatic area was complicated due to little difference in chemical shift between the carbons (2', 3', 8, 1). Thus, the signals of the aromatic carbons were characterized in agreement with Ramos et al.'s work [10] who assigned all of the carbons in novel ester derivatives of rhodamine B in ^{13}C NMR spectra by HETCOR and COLOC measurements.

The aromatic peaks of RBS in the ^1H NMR spectrum were identified by HH COSY measurement (Fig. 5). The measured distance between the hydrogens is 2.489 \AA (Scheme 2). Two triplets with chemical shift 7.6 ppm, assigned to H(I) and H(J) hydrogens, interact with H(H) and H(K) (Scheme 3). The triplet assigned to H(I) has a slightly lower chemical shift than that of H(J). At 6.4 ppm a doublet corresponding to the H(M) hydrogen appears. The peak at 6.7 ppm was assigned to the H(L) hydrogen, by its interaction corresponding to H(M) hydrogen, while the measured distance from the simulations is 2.449 \AA . For the hydrogen in the H(N) position no interactions are inferred by the HH COSY spectrum.

Fig. 6 shows the UV–vis spectra of RB and RBS in ethanol. The absorption maxima of both molecules were

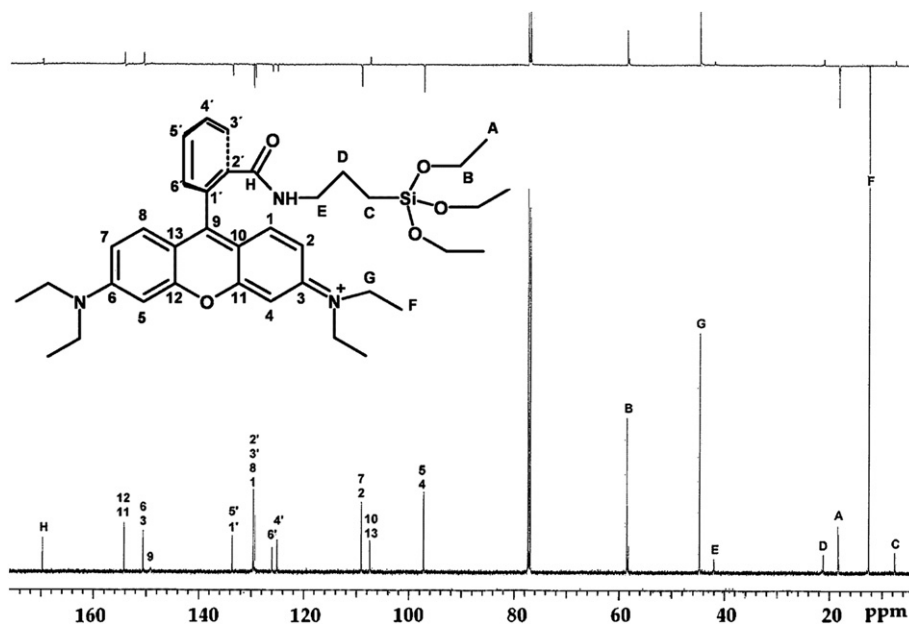


Fig. 4. ^{13}C NMR spectrum of RBS in CDCl_3 .

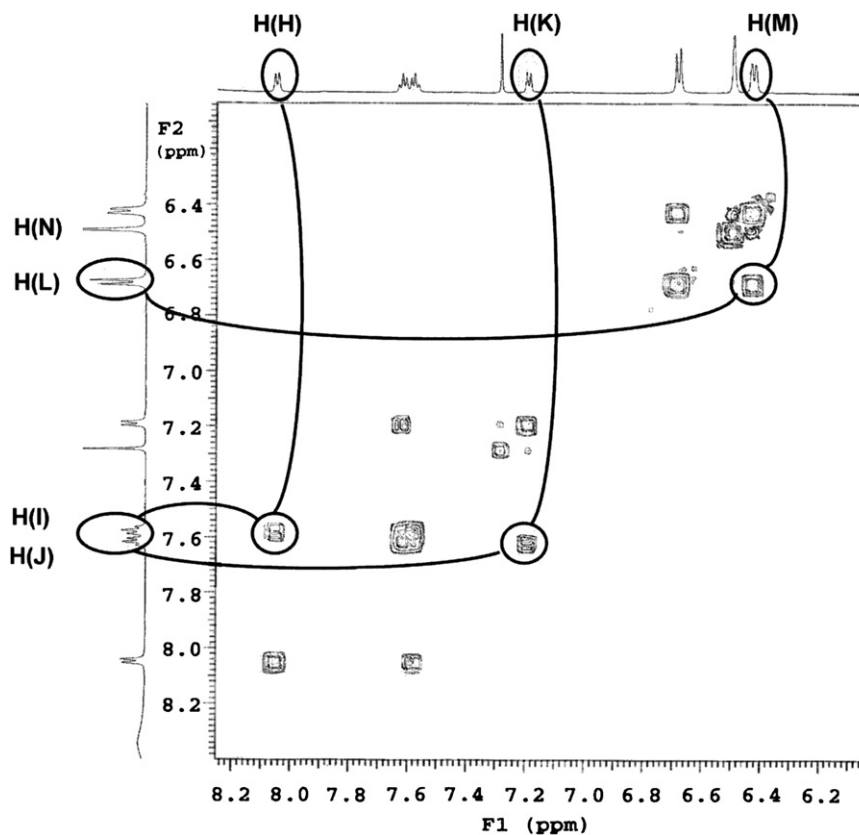
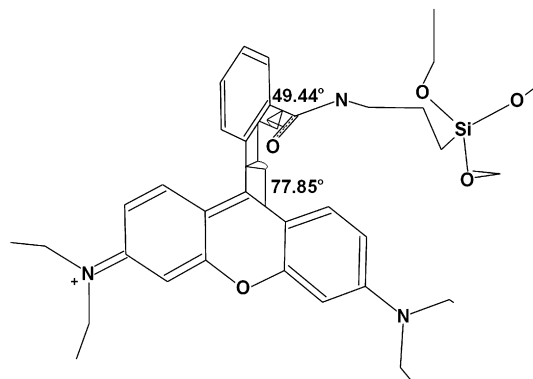


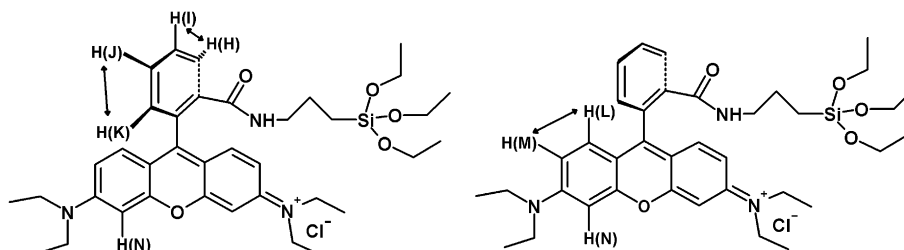
Fig. 5. HH COSY spectrum of RBS, area from 6.3 to 8.4 ppm measured in CDCl_3 .

544.5 nm; the extinction coefficient of RB measured by Houghten et al. [22] was $88\,000\text{ cm}^{-1}\text{ mol}^{-1}\text{ dm}^3$ which was confirmed by our measurements and the extinction coefficient of RBS was found to be $142\,000\text{ cm}^{-1}\text{ mol}^{-1}\text{ dm}^3$. The absorbance of RBS was 1.6 times higher than that of RB which was supported by the molecular simulations. From geometric measurements, an angle of 77.85° between the phthalide and xanthene moieties infers a more planar structure (Scheme 2) than described by Ilich et al. [15], which may be due to the large silane group. The greater conjugation of the phthalide ring with the xanthene ring may have caused the increased extinction coefficient observed in the UV–vis spectra.

The absorption and the fluorescence emission spectra of RB (Fig. 7) and the RBS (Fig. 8) were measured at room temperature in ethanol. Stokes shifts ($\Delta\lambda = \lambda_{\text{em}} - \lambda_{\text{ab}}$), determined on the basis of the spectra, were ($\Delta\lambda = 32.5\text{ nm}$) for RB and



Scheme 2. Diagram of RBS showing the equilibrium conformer geometry. The main torsional angles are indicated.



Scheme 3. Interactions of aromatic hydrogens of RBS measured by HH COSY.

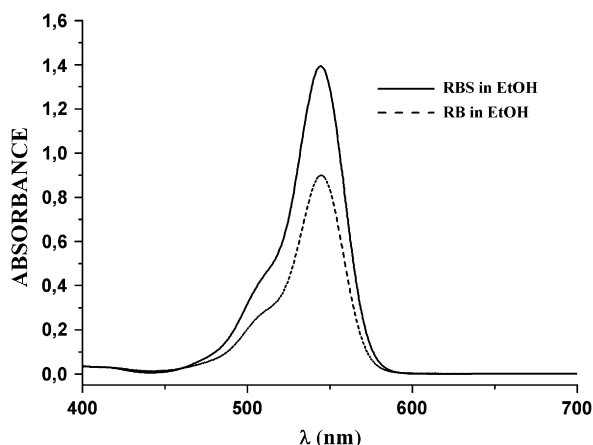


Fig. 6. UV absorption spectra of RBS ($\epsilon = 142\,000\text{ cm}^{-1}\text{ mol}^{-1}\text{ dm}^3$) and RB ($\epsilon = 88\,000\text{ cm}^{-1}\text{ mol}^{-1}\text{ dm}^3$) with absorption maximum (λ_{ab}) at 544.5 nm of concentration $10^{-5}\text{ mol dm}^{-3}$ in EtOH.

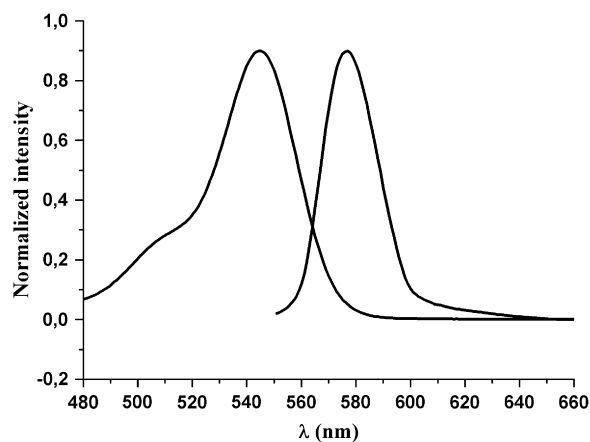


Fig. 7. UV absorption and fluorescence emission spectra of RB in EtOH ($10^{-5}\text{ mol dm}^{-3}$).

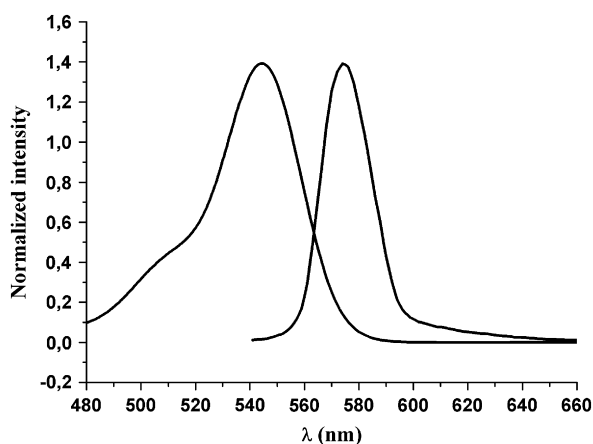


Fig. 8. UV absorption and fluorescence emission spectra of RBS in EtOH ($10^{-5}\text{ mol dm}^{-3}$).

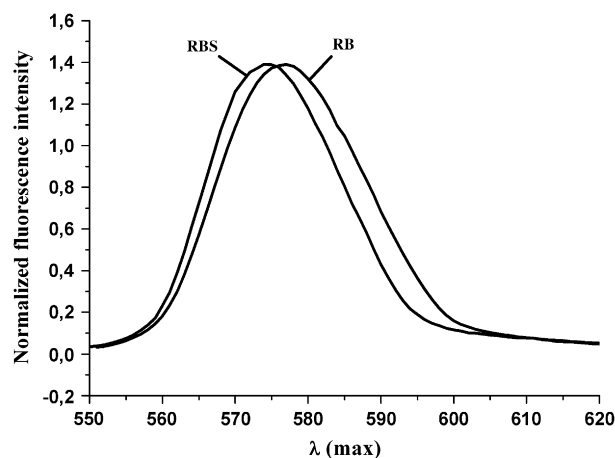


Fig. 9. Fluorescence emission spectra of RBS and RB in EtOH ($10^{-5}\text{ mol dm}^{-3}$).

($\Delta\lambda = 29.5\text{ nm}$) for RBS. The fluorescence emission spectra of RB and RBS are shown in Fig. 9. The binding of APTES to RB perturbs the resonance between the carbonyl group and phthalide moiety, which results in a blue-shift due to the energy increase between the S_0 and S_1 states [36]. The torsion angle of the carbonyl on the phthalide part of RBS, which is strongly out of plane, was 49.44° (Scheme 2) and lends support to this view. In the case of RB, the measurements indicated a planar structure for the carboxyl phthalide group. Fluorescence maxima of RB ($\lambda_{em} = 577\text{ nm}$) and RBS ($\lambda_{em} = 574\text{ nm}$) are given in Table 2.

Furthermore, as implied from our calculations, the molecule favours a *gauche* conformation of the xanthene and phthalide parts of the molecule. The xanthene part is mostly rigid, with freely rotating alkyl-amino groups. The energy barrier for rotation of the alkyl-amines was estimated to be 7–9 kcal/mol, while the rotation of the phthalide group is energetically 5 times greater, stabilizing the *gauche* conformation of the equilibrium conformer.

4. Conclusions

A new kind of rhodamine B with an alkoxyisilane moiety was synthesized via the nucleophilic substitution reaction of 3-aminopropyltriethoxysilane (APTES) and rhodamine B (RB). The structure was characterized by means of the FTIR, ^1H NMR, HH COSY, ^{13}C NMR and UV–vis measurements. The azotropic distillation of water formed in this reaction leads to a pure RBS without need of further purification. The absorbance of RBS was found to be 1.6 times higher than that of RB which was supported by molecular simulations.

Table 2

The extinction coefficient (ϵ), the absorption maxima (λ_{ab}), the emission maxima (λ_{em}) and Stokes shifts ($\Delta\lambda$) of the RB and the RBS in EtOH ($10^{-5}\text{ mol dm}^{-3}$)

	$\epsilon\text{ (cm}^{-1}\text{ mol}^{-1}\text{ dm}^3\text{)}$	$\lambda_{ab}\text{ (nm)}$	$\lambda_{em}\text{ (nm)}$	$\Delta\lambda\text{ (nm)}$
RB	88 000	544.5	577	32.5
RBS	142 000	544.5	574	29.5

However, the observed decreased Stokes shift can be attributed to perturbed resonance between the carbonyl group and the phthalide moiety of the RBS. Further investigations of the covalent binding of RBS into a silica matrix and the physical properties of the dye in the host materials will be published in a forthcoming paper.

Acknowledgements

This work is supported by the Internal Grant of Polymer Institute (SAS) for Young Scientists and VEGA Grant No. 2/6114/26.

References

- [1] Zollinger H. Color chemistry. Syntheses, properties and applications of organic dyes and pigments. 2nd revised ed. Weinheim: VCH; 1991.
- [2] Noelting E, Dziewonski K. Zur Kenntniss der Rhodamine. *Ber* 1905;38:3516–27.
- [3] Ramette RW, Sandell EB. Rhodamine B equilibria. *J Am Chem Soc* 1956;78:4872–8.
- [4] Karpiuk J, Grabowski ZR, De Schryve FC. Photophysics of the lactone form of rhodamine 101. *J Phys Chem* 1994;98:3247–56.
- [5] Drexhage KH. Fluorescence efficiency of laser dyes. *J Res Natl Bur Stand Sec A* 1976;80:421–8.
- [6] Guo Y, Hu Ch, Jiang Ch, Yang Y, Jiang S, Li X, et al. Preparation and heterogeneous photocatalytic behaviors of the surface-modified porous silica materials impregnated with monosubstituted keggins units. *J Catal* 2003;217:141–51.
- [7] Rosenthal I, Peretz P, Muszkat KA. Thermochromic and hyperchromic effects in rhodamine B solutions. *J Phys Chem* 1979;83:350–3.
- [8] Arbeloa IL, Ojeda PR. Molecular forms of rhodamine B. *Chem Phys Lett* 1981;79:347–50.
- [9] Arbeloa IL, Rohatgi-Mukherjee KK. Solvent effect on photophysics of the molecular forms of rhodamine B. Solvation models and spectroscopic parameters. *Chem Phys Lett* 1986;128:474–9.
- [10] Ramos SS, Vilhena AF, Santos L, Almeida P. ^1H and ^{13}C NMR spectra of commercial rhodamine ester derivatives. *Magn Reson Chem* 2000;38:475–8.
- [11] Schaefer EP, Schmidt W, Marth K. New dye lasers covering the visible spectrum. *Phys Lett* 1967;24A:280–1.
- [12] McFarland BB. Laser second-harmonic-induced simulated emission of organic dyes. *Appl Phys Lett* 1967;10:208–9.
- [13] Peterson OG, Snavely BB. Stimulated emission from flash-excited organic dyes in polymethyl methacrylate. *Appl Phys Lett* 1968;12:238–40.
- [14] Tuccio SA, Strome FC. Design and operation of a tunable continuous dye laser. *Appl Opt* 1972;11:64–73.
- [15] Ilich P, Mishra PK, Macura S, Burghardt TP. Direct observation of rhodamine dimer structures in water. *Spectrochim Acta Part A* 1996;52:1323–30.
- [16] Wong MM, Schelly ZA. Solvent-jump relaxation kinetics of the association of rhodamine type laser dyes. *J Phys Chem* 1974;78:1891–5.
- [17] Sauer K, Smith JRL, Schulta AJ. The dimerization of chlorophyll *a*, chlorophyll *b*, and bacteriochlorophyll in solution. *J Am Chem Soc* 1966;88:2681–8.
- [18] McKay RB, Hilson PJ. Metachromatic behaviour of dyes in solvents of high dielectric constant: the anomaly of water. *Trans Faraday Soc* 1967;63:777–81.
- [19] Monahan AR, Blossey DF. Aggregation of arylazonaphthols. I. Dimerization of Bonadur Red in aqueous and methanolic systems. *J Phys Chem* 1970;74:4014–21.
- [20] Hana XM, Lina J, Xingb RB, Fub J, Wanga SB. Patterning and optical properties rhodamine B-doped organic–inorganic silica films fabricated by sol–gel soft lithography. *Mater Lett* 2003;57:1355–60.
- [21] Du H, Fuh RA, Li J, Corkan A, Lindsey JS. A computer-aided design and research tool in photochemistry. *Photochem Photobiol* 1998;68:141–2.
- [22] Houghten RA, Dooley CT, Appel JR. De novo identification of highly active fluorescent kappa opioid ligands from a rhodamine labeled tetrapeptide positional scanning library. *Bioorg Med Chem Lett* 2004;14:1947–51.
- [23] Carl EA, Wimpfheimer H. Thickness measurement of silicon dioxide layers by ultraviolet–visible interference method. *Solid-State Electron* 1964;7:755–61.
- [24] Karolin J, Bogen ST, Johansson BA, Molotkovsky JG. Polarized fluorescence and absorption spectroscopy of 1,3,2-dihydroxy-dotriacontane-bis-rhodamine 101 ester. A new and lipid bilayer-spanning probe. *J Fluoresc* 1995;5:279–85.
- [25] Hinkley DA, Saybold PG, Borris DP. Solvatochromism and thermochromism of rhodamine solutions. *Spectrochim Acta Part A Mol Spectrosc* 1986;42:747–54.
- [26] Mandal K, Pearson TDL, Demas JN. Lumineszenzspektrometrie; Organ. Farbstoffe in PVA oder PVP. *Anal Chem* 1980;52:2184–9.
- [27] Moser JG. Photodynamic tumor therapy: 2nd and 3rd generation photosensitizers. Australia: Harwood Academic Publishers; 1998.
- [28] Ma YJ, Zhou M, Jin XY, Zhang BZ, Chen H, Guo NY. Flow-injection chemiluminescence determination of ascorbic acid by use of the cerium(IV)–rhodamine B system. *Anal Chim Acta* 2002;464:289–93.
- [29] Chen H, Zhou M, Jin XY, Song YM, Zhang ZY, Ma YJ. Chemiluminescence determination of ultramicro DNA with a flow-injection method. *Anal Chim Acta* 2003;478:31–6.
- [30] Roy BC, Peterson R, Mallik S, Campiglia AD. Synthesis and fluorescence properties of new, fluorescent, polymerizable, metal-chelating lipids. *J Org Chem* 2000;65:3644–51.
- [31] Ficht S, Roeglin L, Ziehe M, Breyer D, Seitz O. Direct carbodiimide-mediated conjugation of carboxylates using pyridinium *p*-toluenesulfonate and tertiary amines as additives. *Synth Lett* 2004;14:2525–9.
- [32] Shukla V, Mishra S, Watal G, Misra K. Design, development and synthesis of a novel labeled PNA monomer incorporated in DNA-hexamer to act as a hybridization probe by FRET. *Indian J Chem Sect B* 2005;44:121–9.
- [33] Ohishi T. An ethoxy-silano rhodamine B derivative and its application to surface coatings on display devices. *J Non-Cryst Solids* 2003;332:80–6.
- [34] Dewar MJS, Thiel W. Ground states of molecules. 38. The MNDO method. Approximations and parameters. *J Am Chem Soc* 1977;99:4899–907.
- [35] Dewar MJS, Zoebisch EG, Healy EF, Stewart JJP. Development and use of quantum mechanical molecular models. 76. AM1: a new general purpose quantum mechanical molecular model. *J Am Chem Soc* 1985;107:3902–9.
- [36] Kim HS, Cho Bae, Kwon JY, Kim SK, Choi M, Yoon J. Study on the fluorescence of 1,8-anthracenedicarboxylic acid and 1,8-anthracenediformamide. *Bull Korean Chem Soc* 2001;22:929–31.